Impact of Electric Vehicle Aggregator with Communication Time Delay on Stability Regions and Stability Delay Margins in Load Frequency Control System

Ausnain Naveed, Şahin Sönmez, and Saffet Ayasun

***Abstract*—This paper investigates the impact of electric vehicle (EV) aggregator with communication time delay on stability regions and stability delay margins of a single-area load frequency control (LFC) system. Primarily, a graphical method characterizing stability boundary locus is implemented. For a given time delay, the method computes all the stabilizing proportional-integral (PI) controller gains, which constitutes a stability region in the parameter space of PI controller. Secondly, in order to complement the stability regions, a frequency-domain exact method is used to calculate stability delay margins for various values of PI controller gains. The qualitative impact of EV aggregator on both stability regions and stability delay margins is thoroughly analyzed and the results are authenticated by time-domain simulations and quasi-polynomial mapping-based root finder (QPmR) algorithm.**

***Index Terms*—Communication time delay, electric vehicle (EV) aggregator, frequency regulation, proportional-integral (PI) controller design, stability delay margin, stability region.**

I. Introduction

LOAD frequency control (LFC) systems aim to regulate the frequency and to keep the scheduled tie-line power exchange in an interconnected power system with independently controlled multiple areas [1]. Due to the increasing environmental concerns, the gradual depletion of fossil resources and the increased penetration of highly variable renewable energy (RE) power generation, frequency control and stability are becoming more and more important [2]. Electric vehicles (EVs) with vehicle-to-grid (V2G) technology have become a promising tool that can mitigate the intermittent effects of RE sources and regulate the system frequency. This is due to the fact that batteries in EVs can quickly adjust the power output as compared with conventional generators. This quick response characteristic increases the dynamic performance of LFC systems. EVs can be operated as loads or generators. Therefore, they reduce fluctuations in demand or generation and improve frequency response [3]-[6]. For the practical participation of EVs in frequency regulation market, a new entity, i.e., EV aggregator, is required to aggregate and control a large number of EVs in order to satisfy the frequency regulation criteria [7]-[10]. The main function of an EV aggregator is to send and receive the information regarding the charging status of EVs and their available electric power and energy capacities to LFC center, and to rearrange the control signals dispersing EVs in order to adjust their power output using an automatic generation control (AGC).

For the AGC system, EV aggregator requires a dedicated or an open communication network to transfer the control commands to EVs. The latter is preferred due to its low cost, but it is prone to time delays in the communication network [11]-[13]. These delays can adversely affect the dynamics of LFC system and its stability against the expectation that EVs can enhance the dynamic performance of LFC [14], [15]. Therefore, it is important to investigate the delay-dependent stability of LFC systems enhanced by EVs denoted as LFC-EVs, and to compute the stability delay margins defined as the allowable upper bound on the communication time delay. Besides, the determination of all parameters of the stabilizing proportional-integral (PI) controller is required to guarantee the stability of LFC-EVs in the presence of communication delays.

Even though the EVs are widely used in future smart grid, the reported research that studies the impact of both communication delay and the integration of EVs on the frequency regulation is very limited. For example, in [14], an indirect method based on Lyapunov stability theory with linear matrix inequalities (LMIs) has been implemented to calculate stability delay margins of a single-area LFC-EVs. In [15], a combination of frequency sweeping test and the binary iteration algorithm is used to compute the stability delay margins of single-area LFC-EV system for different load sharing scenarios between conventional generator and EV ag-

Manuscript received: April 12, 2019; accepted: January 13, 2020. Date of CrossCheck: January 13, 2020. Date of online publication: July 22, 2020.

This work was supported by the Project of Scientific and Technological Research Council of Turkey (TUBITAK) (No. 118E744).

A. Naveed, S. Sönmez, and S. Ayasun (corresponding author) are with the Department of Electrical and Electronic Engineering, Niğde Ömer Halisdemir University, Niğde, Turkey, and S. Ayasun is also with the Department of Electrical and Electronic Engineering, Gazi University, Ankara, Turkey (e-mail: husnain.naveed@gmail.com; sahinsonmez@ohu.edu.tr; saffetayasun@gazi.edu.tr).

DOI: 10.35833/MPCE.2019.000244

gregator. The time-domain method in [14] gives more conservative stability delay margin results than the frequency-domain methods. The frequency sweeping test in [15] also gives exact delay margins. However, the selection of the frequency range for the sweeping test requires undesired computation effort.

In frequency regulation service, the response time to the regulation command from independent system operator (ISO) is critical. In general, the aggregator receives a regulation command from ISO every 2 to 6 s [16]. ISOs usually have their own communication requirements for the maximum allowed delay to respond to their regulation signals. For example, the requirement of California ISO for the communication time delay between the aggregator and EVs is to be within 4 s [17]. For any given communication delay limit imposed by the ISO, it is essential to determine all stabilizing PI controller gains for a stable operation of LFC-EV systems.

This paper presents an efficient analytical method to compute all stabilizing PI controller parameters, which constitute a stability region of a single-area LFC-EV system in the parameter space of controller with communication delay. The technique relies on the stability boundary locus that can be simply obtained by equating the imaginary and real parts of the characteristic equation of LFC-EV system to zero [18]. The suggested method has been effectively applied to a single-area and two-area LFC system containing single delay without EVs, respectively [19], [20]. In this paper, stability regions are obtained using various delay values and load sharing schemes to evaluate the effect of EV aggregator and time delay.

In addition to stability regions, a frequency-domain direct method based on the removal of the exponential terms [21] in the characteristic equation of the LFC-EV system is also implemented to determine stability delay margins. The proposed technique is an exact method and has been effectively utilized for the delay-dependent stability investigation of conventional LFC system without the inclusion of EVs [22]. The impacts of EVs and controller gains on stability delay margins are thoroughly investigated.

Time-domain simulations [23] along with an independent algorithm, i. e., quasi-polynomial mapping-based root finder (QPmR) algorithm [24], are used to validate the correctness of the boundaries of stability regions and the exactness of stability delay margin results. This root finder algorithm is a mathematical approach for calculating the spectrum of zeros of quasi-polynomials in the *s*-plane.

This paper presents a comprehensive delay-dependent stability analysis of a single-area LFC-EV system and makes the following main contributions.

1) Identification of stability regions in the parameter space of PI controller using stability boundary locus method. With the help of stability regions, one can easily adjust PI controller gains that will ensure the stability of LFC-EV system and reduce the adverse effect of communication delays on frequency regulation.

2) Computation of stability delay margins for a wide range of PI controller gains using a frequency-domain exact method. Stability delay margins are expected to guide the determination of communication and delay requirements for EV aggregators participating in frequency regulation service for a given PI controller.

3) Verification of stability regions and delay margins by an independent algorithm. The QPmR algorithm clearly proves the effectiveness and accuracy of the stability boundary locus method used for obtaining stability regions and the frequency-domain direct method for computing stability delay margins.

II. Single-area LFC System Model with EV Aggregator

To utilize EVs in frequency regulation, numerous EVs are required to be plugged into the power grid. An EV aggregator is a control center of EVs, which manages the charging and discharging behavior of each EV in an aggregator. The dynamic model of the i^{th} EV in the EV aggregator is described by the following first-order transfer function [14], [15]:

$$G_{EV,i}(s)=\frac{K_{EV,i}}{1+sT_{EV,i}} \tag{1}$$

where $K_{EV,i}$ and $T_{EV,i}$ are the gain and time constants of the i^{th} EV battery system, respectively.

The communication delay from an EV aggregator to the i^{th} EV and the scheduling delay in the EV aggregator is generally lumped and modeled by a transfer function of $e^{-s\tau_i}$, where τ_i is the delay time taken for receiving control signals from the EV aggregator. The delays τ_i for all EVs and the time constants $T_{EV,i}$ ($i=1, 2, ..., N$) are assumed to be equal in an average sense, denoted by τ and T_{EV}, respectively. With the assumption, an aggregated model of several EVs consisting of one delay function and one EV dynamics is obtained. The use of an aggregated model of EV fleet seems to be reasonable since a cluster of numerous EVs as well as traditional generators are controlled together to change their power injection to follow the load disturbances [25], [26].

The block diagram of a single-area LFC system including an EV aggregator and delay block is presented in Fig. 1 [14].

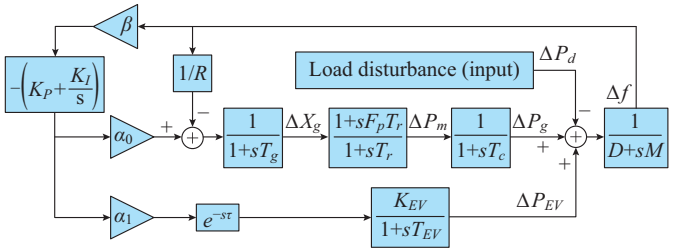

Fig. 1. System model of single-area LFC with EV aggregator.

The PI type controller is adopted as LFC controller. In Fig. 1, Δf, ΔX_g, ΔP_m, ΔX_g, ΔP_{EV} and ΔP_d are the deviation of frequency, valve position, mechanical power output, generator power output, EV aggregator power output and load disturbance, respectively; D, M, R, β, F_p, T_g, T_r and T_c are the damping coefficient, generator inertia constant, speed drop,

frequency bias factor, fraction of the total turbine power, time constant of the governor, reheat and turbine, respectively; and K_P and K_I are the PI controller gains. Because of any sudden changes in load demand, the area control error *ACE* as a control signal is transmitted to the PI controller and then the output signal of the PI controller is sent to the reheat steam turbine and the EV aggregator based on their participation factors α_0 and α_1 for regulating the system frequency. The control signals transmitted to the EV aggregator through the communication networks ensure that the EV aggregator participates in frequency regulation service to the grid.

It should be noted that communication delays observed in the transmission of regulation signal from ISO to the conventional generators are not considered in this study, since the delays from EV aggregators to EVs are more significant [12], [14], [15]. One reason for this assumption is that the communication link between ISO and conventional generators is generally deployed by the ISO itself and communication delay requirements of this link is ensured by ISO. Another reason is the utilization of open communication links between EV aggregator and EVs. These links include wireless mobile communication networks, Internet, power line communication (PLC), WiFi, and ZigBee depending on the geographical distribution of EVs. Such communication networks cause significant delays as compared with those observed between ISO and power plants. Moreover, there exist scheduling delays since EV aggregators have to control both charging and regulation of a large number of EVs [12], [25]. Additionally, [14] has shown that the stability and frequency regulation of LFC systems are more severely affected by the communication delays in fast-response resources such as EVs, compared with those in conventional generators, when EVs with communication network delays participate in frequency regulation service.

For stability region and delay margin computations, it is necessary to obtain the characteristic equation of the single-area LFC-EV system. This could be easily obtained from Fig. 1 as the following equation:

$$\Delta(s,\tau)=P(s)+Q(s)\mathrm{e}^{-s\tau}=0 \tag{2}$$

where $\Delta(s,\tau)$ is the characteristic equation; and $P(s)$ and $Q(s)$ are the two polynomials with real coefficients in terms of system parameters. These polynomials are:

$$\begin{cases} P(s)=p_6s^6+p_5s^5+p_4s^4+p_3s^3+p_2s^2+p_1s+p_0 \\ Q(s)=q_4s^4+q_3s^3+q_2s^2+q_1s+q_0 \end{cases} \tag{3}$$

The coefficients of $P(s)$ and $Q(s)$ polynomials depend on the LFC-EV system parameters and PI controller gains. Those coefficients are given in (A1) and (A2) in Appendix A.

III. Computation of Stability Regions

To identify the boundary of the stability region in the parameter space of PI controller, (K_P,K_I)-plane for a given time delay τ, $s=\mathrm{j}\omega_c$ and the crossing frequency $\omega_c>0$ is substituted into (2). The PI controller gains are then separated to obtain a new equation as follows [17]-[19]:

$$\begin{aligned} \Delta(\mathrm{j}\omega_c,\tau)=&\,p_6(\mathrm{j}\omega_c)^6+p_5(\mathrm{j}\omega_c)^5+p_4(\mathrm{j}\omega_c)^4+\bar{p}_3(\mathrm{j}\omega_c)^3+\\ &\bar{p}_2(\mathrm{j}\omega_c)^2+\bar{p}_1(\mathrm{j}\omega_c)+K_P\left(p_3'(\mathrm{j}\omega_c)^3+p_2'(\mathrm{j}\omega_c)^2+p_1'(\mathrm{j}\omega_c)\right)+\\ &K_P\left(q_4'(\mathrm{j}\omega_c)^4+q_3'(\mathrm{j}\omega_c)^3+q_2'(\mathrm{j}\omega_c)^2+q_1'(\mathrm{j}\omega_c)\right)\mathrm{e}^{-\mathrm{j}\omega_c\tau}+\\ &K_I\left(p_2''(\mathrm{j}\omega_c)^2+p_1''(\mathrm{j}\omega_c)+p_0''\right)+\\ &K_I\left(q_3''(\mathrm{j}\omega_c)^3+q_2''(\mathrm{j}\omega_c)^2+q_1''(\mathrm{j}\omega_c)+q_1''\right)\mathrm{e}^{-\mathrm{j}\omega_c\tau}=0 \end{aligned} \tag{4}$$

It should be noted that p_6, p_5 and p_4 coefficients in (4) are those given in (3) and (A1), and that the coefficients of $\bar{p}_1$, $\bar{p}_2$ and $\bar{p}_3$ represent the terms of p_1, p_2 and p_3, respectively in (A1) that do not contain K_P and K_I. On the other hand, p' and q' coefficients in (4) corresponds to the remaining terms of p and q containing K_P in (A1), respectively, after K_P is extracted from them, while p'' and q'' coefficients in (4) corresponds to the remaining terms of p and q, respectively, including K_I in (A1) after K_I is extracted from them.

Substituting $\mathrm{e}^{-\mathrm{j}\omega_c\tau}=\cos(\omega_c\tau)-\mathrm{j}\sin(\omega_c\tau)$ into (4) and separating the imaginary and real parts, a more compact form of (4) is obtained as:

$$\begin{cases} \Delta(\mathrm{j}\omega_c,\tau)=K_PA_1(\omega_c)+K_IB_1(\omega_c)+C_1(\omega_c)+\\ \qquad\qquad \mathrm{j}\left(K_PA_2(\omega_c)+K_IB_2(\omega_c)+C_2(\omega_c)\right)=0 \\ \Delta(\mathrm{j}\omega_c,\tau)=\Re\left\{\Delta(\mathrm{j}\omega_c,\tau)\right\}+\mathrm{j}\Im\left\{\Delta(\mathrm{j}\omega_c,\tau)\right\}=0 \end{cases} \tag{5}$$

where $\Re\{\cdot\}$ and $\Im\{\cdot\}$ represent the real and imaginary parts of the characteristic equation, respectively. Moreover, the expressions for A_1, B_1, C_1, A_2, B_2 and C_2 are given in (A3) and (A4).

Setting both the imaginary and real parts of $\Delta(\mathrm{j}\omega_c,\tau)=0$ in (5) to zero, the following equations are obtained:

$$\begin{cases} K_PA_1(\omega_c)+K_IB_1(\omega_c)+C_1(\omega_c)=0 \\ K_PA_2(\omega_c)+K_IB_2(\omega_c)+C_2(\omega_c)=0 \end{cases} \tag{6}$$

Equation (6) is solved for (K_P,K_I) to identify the stability boundary locus $\ell(K_P,K_I,\omega_c)$ in the (K_P,K_I)-plane shown as:

$$\begin{cases} K_P=\dfrac{B_1(\omega_c)C_2(\omega_c)-B_2(\omega_c)C_1(\omega_c)}{A_1(\omega_c)B_2(\omega_c)-A_2(\omega_c)B_1(\omega_c)} \\ K_I=\dfrac{A_2(\omega_c)C_1(\omega_c)-A_1(\omega_c)C_2(\omega_c)}{A_1(\omega_c)B_2(\omega_c)-A_2(\omega_c)B_1(\omega_c)} \end{cases} \tag{7}$$

This stability boundary obtained by (6) is called as complex root boundaries (CRBs) of the LFC-EV system. It is noted that a real root of (2) may cross the jω-axis across the origin. Moreover, it can be observed from (5) and (A3) that such a stability change occurs only for $K_I=0$, defining another boundary called as real root boundary (RRB) locus. As a result, the (K_P,K_I)-plane is divided into stable and unstable regions by the RRB locus $K_I=0$ and the CRB locus $\ell(K_P,K_I,\omega_c)$ determined by (7).

IV. Computation of Stability Delay Margins

The aim of studying the stability of time-delayed system is to determine whether the stability is delay-dependent or delay-independent. For the former type, the system remains stable for $\tau<\tau^*$, where τ^* is the stability delay margin. However, the system becomes unstable when the delay exceeds

the margin, i.e., $\tau > \tau^*$. Whereas, in the latter case, the system remains stable for all finite values of time delays. The stability delay margin is the basic requirement for the stability assessment of LFC-EV systems and it should always be more than the total time delays observed in the system. In order to assess the stability of the single-area LFC-EV system shown in Fig. 1, it is necessary to have information on stability delay margins for a wide range of system parameters.

The necessary condition for the single-area LFC-EV system to be asymptotically stable is that all the roots of (2) must be in the left half of the s-plane. In consideration of the single delay, the delay margin computation can be done by finding values of τ^* for which (2) has roots (if any) on the jω-axis. Here, $\Delta(s,\tau)=0$ is an implicit function of s and τ that may or may not cross the jω-axis. To simplify the task, it is assumed that $\Delta(s,0)=0$ has all the roots placed in the left half plane, that is, the system with no delay is already stable. Note that (2) has an exponential term $e^{-s\tau}$ that results in infinitely many finite roots. This makes the computation of the roots and stability delay margin a challenging problem. However, the determination of these infinite numbers of roots is not necessary for delay-dependent stability assessment of the LFC-EV system. The roots located on the jω-axis and the corresponding delay value are required to be determined. If, for some finite value of τ^*, the characteristic polynomial of $\Delta(s,\tau^*)=0$ has a root on the imaginary axis at $s=\mathrm{j}\omega_c$, the equation of $\Delta(-s,\tau^*)=0$ will also have the same root on the imaginary axis for the same value of τ^* and ω_c due to the complex conjugate symmetry of complex roots. That means $s=\mathrm{j}\omega_c$ will be a common root of the following equation:

$$\begin{cases}\Delta(s,\tau^*)=P(\mathrm{j}\omega_c)+Q(\mathrm{j}\omega_c)\mathrm{e}^{-\mathrm{j}\omega_c\tau^*}=0\\ \Delta(-s,\tau^*)=P(-\mathrm{j}\omega_c)+Q(-\mathrm{j}\omega_c)\mathrm{e}^{\mathrm{j}\omega_c\tau^*}=0\end{cases} \tag{8}$$

By eliminating the exponential terms between the two subequations in (8), the following augmented polynomial is obtained:

$$W(\omega_c^2)=P(\mathrm{j}\omega_c)P(-\mathrm{j}\omega_c)-Q(\mathrm{j}\omega_c)Q(-\mathrm{j}\omega_c)=0 \tag{9}$$

By substituting the polynomials of $P(\mathrm{j}\omega_c)$, $P(-\mathrm{j}\omega_c)$, $Q(\mathrm{j}\omega_c)$ and $Q(-\mathrm{j}\omega_c)$ into (9), the augmented polynomial of $W(\omega_c^2)$ can be represented as:

$$W(\omega_c^2)=t_{12}\omega_c^{12}+t_{10}\omega_c^{10}+t_8\omega_c^8+t_6\omega_c^6+t_4\omega_c^4+t_2\omega_c^2+t_0=0 \tag{10}$$

where $t_{12}=p_6^2$; $t_{10}=p_5^2-2p_6p_4$; $t_8=p_4^2+2p_6p_2-2p_5p_3-q_4^2$; $t_6=p_3^2-2p_6p_0-2p_4p_2+2p_5p_1+2q_4q_2-q_3^2$; $t_4=p_2^2+2p_4p_0-2p_3p_1-2q_4q_0+2q_3q_1-q_2^2$; $t_2=p_1^2-2p_2p_0+2q_2q_0-q_1^2$; and $t_0=p_0^2-q_0^2$.

It is observed that the characteristic equation of (2) with exponential terms is now converted into a polynomial (10) without transcendental terms. More importantly, the real positive roots of (10) exactly coincide with the imaginary roots $s=\pm\mathrm{j}\omega_c$ of (2). The roots of (10) can be easily computed using any standard method. The following situations may occur depending on the roots of the new polynomial:

1) The system is stable for all finite delays $\tau \geq 0$, indicating that the system has delay-independent stability. This happens when (10) does not have any positive real roots, which infers that (2) does not have any roots on the jω-axis.

2) The system has delay-dependent stability in the interval of $[0, \tau^*]$. This happens when (10) has at least one positive real root, which infers that (2) has at least one complex roots pair on the jω-axis.

The corresponding value of τ^* for a real positive root ω_c is simply obtained by using (2) as [22], [23]:

$$\tau^*=\frac{1}{\omega_c}\arctan\left(\frac{a_9\omega_c^9+a_7\omega_c^7+a_5\omega_c^5+a_3\omega_c^3+a_1\omega_c}{a_{10}\omega_c^{10}+a_8\omega_c^8+a_6\omega_c^6+a_4\omega_c^4+a_2\omega_c^2+a_0}\right) \tag{11}$$

where $a_{10}=-p_6q_4$; $a_9=-p_6q_3+p_5q_4$; $a_8=p_6q_2-p_5q_3+p_4q_4$; $a_7=p_6q_1-p_5q_2+p_4q_3-p_3q_4$; $a_6=-p_6q_0+p_5q_1-p_4q_2+p_3q_3-p_2q_4$; $a_5=p_5q_0-p_4q_1+p_3q_2-p_2q_3+p_1q_4$; $a_4=-p_3q_1+p_2q_2-p_1q_3+p_0q_4$; $a_3=-p_3q_0+p_2q_1-p_1q_2-p_0q_3$; $a_2=-p_2q_0+p_1q_1-p_0q_2$; $a_1=p_1q_0-p_0q_1$; and $a_0=p_0q_0$.

V. Results

This section presents the stability regions in the parameter space of PI controller, the stability delay margin results for single-area LFC-EVs, and the validation studies employing time-domain simulations and the QPmR algorithm. The system parameters are: $M=8.8$, $D=1$, $T_g=0.2$, $T_c=0.3$, $T_r=12$, $F_P=1/6$, $R=1/11$, $\beta=21$, $K_{EV}=1$, $T_{EV}=0.1$ [14].

A. Stability Region Results

In this subsection, the impact of EV aggregator participation factor α_1 and the communication time delay τ on the stability region is investigated. The stability region in the (K_P, K_I)-plane is firstly obtained without EV aggregator ($\alpha_1=0$). This scheme corresponds to the case where all required control efforts for frequency regulation are provided by the conventional generator ($\alpha_0=1$) and the communication time delay $\tau=0$. The stability region is illustrated in Fig. 2.

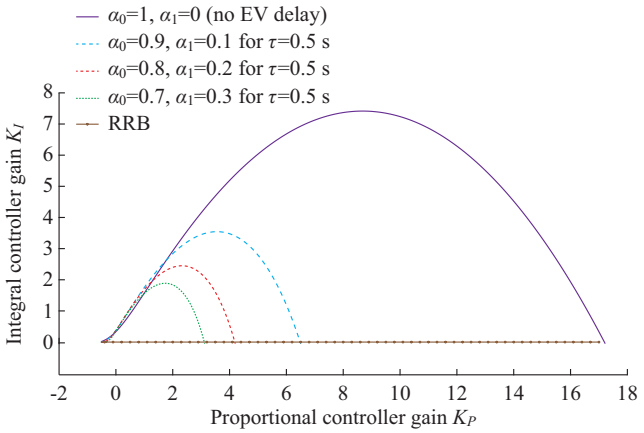

Fig. 2. Stability regions for different values of EV aggregator participation factors ($\tau=0.5$ s).

Then, to investigate the impact of EV aggregator participation factor on the stability region, three different EV aggregator participation factors are selected, i.e., $\alpha_1=0.1$, 0.2 and 0.3, whereas the time delay is fixed at $\tau=0.5$ s. These participation factors imply that 10%, 20% and 30% of the re-

quired control efforts are provided by the EV aggregator with a time delay of $\tau = 0.5$ s. Figure 2 compares the corresponding stability regions. Note that the largest region is observed when EV participation is not considered ($\alpha_1 = 0$). More importantly, the size of stability regions decreases as the EV participation factor increases, whereas the shape of the regions is unchanged. Figure 2 clearly illustrates that the stability regions get smaller as the contribution of EV aggregator to the frequency regulation increases due to the presence of communication time delay.

The impact of time delay is then investigated for a selected EV participation factor. Figure 3 illustrates the stability regions for $\tau = 0.25$ s, 0.5 s, 0.75 s and 1.0 s, when the participation factors are chosen as $\alpha_0 = 0.8$ and $\alpha_1 = 0.2$, respectively. Figure 3 clearly shows that the stability regions shrink as the time delay increases from $\tau = 0.25$ s to $\tau = 1.0$ s, whereas their shapes remain unchanged. The stability regions in Fig. 2 and Fig. 3 illustrate that both EV participation factor and the time delay associated with EV aggregator have significant adverse effect on the stability regions. These stability regions represent a set of all stabilizing PI controller gains which ensures a stable operation of the LFC-EV system.

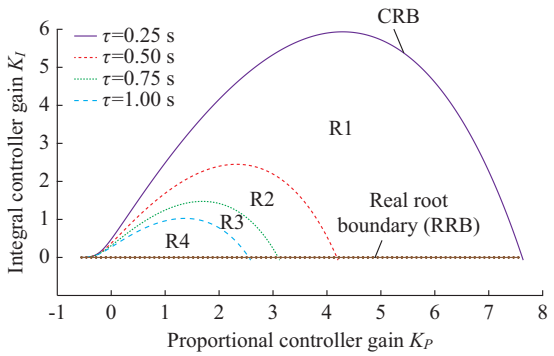

Fig. 3. Stability region for different communication delays for $\alpha_1 = 0.2$.

Finally, the accuracy of stability boundary locus CRB is validated by the time-domain simulations and the QPmR algorithm. The PI controller gains are selected as $K_P = 3.203$, $K_I = 2.0$ on the CRB locus of region R2 illustrated by the dashed-line in Fig. 3.

Figure 4 shows the time-domain simulation along with the QPmR algorithm based dominant root distribution and their zoom picture. It can be seen that the LFC-EV system is marginally stable due to undamped frequency response because of a complex conjugate root pair located on the jω-axis for the selected gains. This implies that the LFC-EV system will be asymptotically stable with decaying oscillation in the frequency response for any PI controller gains inside the region R2. Additionally, the LFC-EV system will become unstable with growing oscillations in frequency for any controller gains outside the region R2.

B. Stability Delay Margin Results

Stability delay margins are computed for a wide range of PI controller gains. The theoretical stability delay margins are shown in Table I for EV participation factor of $\alpha_1 = 0.2$.

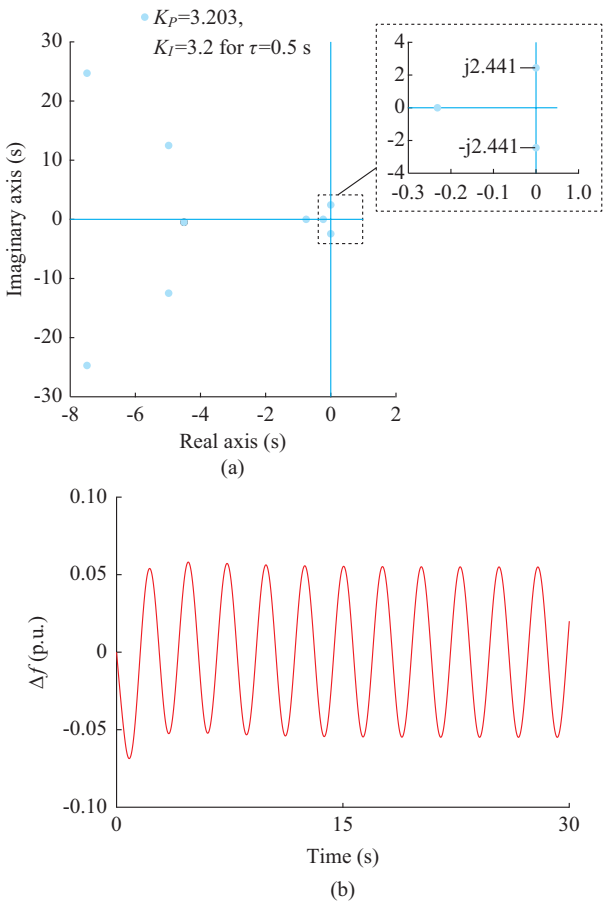

Fig. 4. Dominant root distribution around CRB locus and frequency response for marginally stable case. (a) Root distribution. (b) Frequency response.

TABLE I
RESULTS OF STABILITY DELAY MARGIN τ^* FOR $\alpha_1 = 0.2$

K_P	τ^* (s)				
	$K_I = 0.2$	$K_I = 0.4$	$K_I = 0.6$	$K_I = 0.8$	$K_I = 1.0$
0.0	1.7871	0.4230	0.0857	*	*
0.1	2.7435	0.8269	0.3494	0.1338	0.0131
0.2	3.5876	1.2000	0.6015	0.3239	0.1653
0.3	4.2535	1.5212	0.8325	0.5031	0.3111
0.4	4.6984	1.7766	1.0342	0.6665	0.4474
0.5	4.8590	1.9627	1.2018	0.8104	0.5713
0.6	4.6807	2.0821	1.3332	0.9322	0.6808
0.7	4.3114	2.1423	1.4292	1.0311	0.7746
0.8	3.9029	2.1533	1.4926	1.1074	0.8522
0.9	3.5170	2.1258	1.5266	1.1621	0.9137
1.0	3.1714	2.0700	1.5363	1.1974	0.9600

The results in Table I indicate that for a fixed value of K_P, the stability delay margin decreases when K_I is increased, which infers a less stable system. It is observed that the delay margins are not computed for the values of K_P and K_I such that the delay-free system ($\tau = 0$) is unstable. The corresponding locations are marked by * in Table I. Moreover, the stability delay margin increases with K_P for nearly all

values of K_I. The EV aggregator participation factor should also be investigated for different values of K_P and K_I in order to observe its impact on the stability delay margin. As shown in Fig. 5, the stability delay margins decrease with an increase in EV aggregator participation factor α_1 for $K_P = 0.3$ and $K_I = 0.6$.

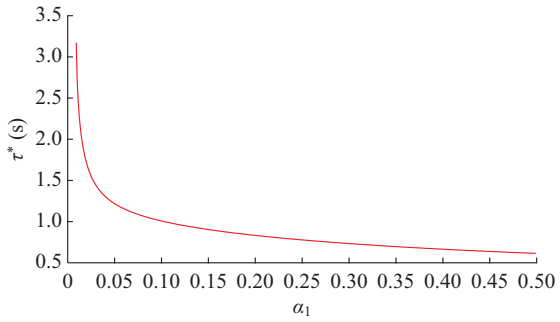

Fig. 5. Variation of stability delay margin regarding EV aggregator participation factor for $K_P = 0.3$ and $K_I = 0.6$.

The theoretical delay margins are verified using time-domain simulations and QPmR algorithm. The controller gains are chosen as $K_P = 0.3$, $K_I = 0.6$, and the EV participation factor $\alpha_1 = 0.2$. It is clear from Table I that the stability delay margin is computed as $\tau^* = 0.8325$ s for this case. The dominant roots distribution of (2) and frequency response of the LFC-EV system for $\tau^* = 0.8325$ s is shown in Fig. 6.

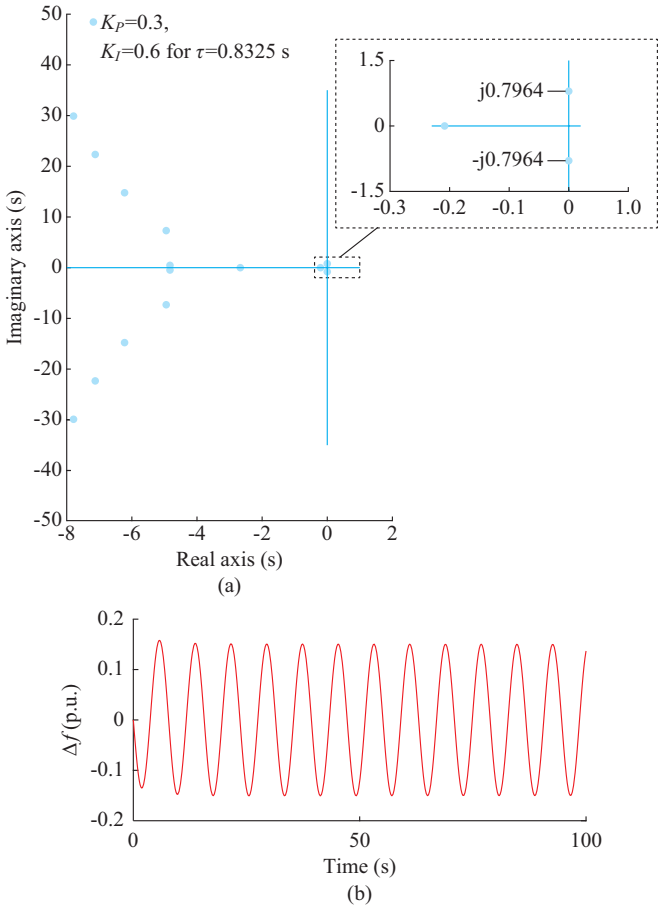

Fig. 6. Dominant root distribution by QPmR algorithm and frequency response for $\tau^* = 0.8325$ s. (a) Root distribution. (b) Frequency response.

Note that the system has a pair of complex roots on the imaginary axis. The frequency response exhibits sustained oscillations which indicate the marginal stability of LFC-EV system. If the time delay exceeds the stability delay margin, the system will become unstable due to the growing oscillations in the frequency response. Figure 6 clearly proves the accuracy of the theoretical stability delay margin.

VI. Conclusion

This paper has presented a comprehensive study on the effect of integrating EV aggregator with communication time delay to conventional LFC system. For a given time delay and load sharing scheme, a set of all stabilizing PI controller gains that constitute a stability region in the parameter space of the controller has been determined using a graphical exact method. The impact of both time delay and EV aggregator participation factor on the stability regions has been evaluated. It is observed that the size of stability regions decreases as the time delay and EV participation factor increase.

To complement stability region results, stability delay margins have been determined for a large number of PI controller gains using a frequency domain exact method. It has been observed that stability delay margin becomes smaller with an increase in the integral gain. Moreover, for any given PI controller gains, an increase in EV aggregator participation factor results in a decrease in stability delay margin. If the PI controller gains and participation factor of EVs are not properly selected, the EV aggregator participation with a communication time delay may cause instability and degrade the dynamic response against an expectation that EVs can improve the LFC dynamic performance.

It is expected that the results will allow us to determine the communication delay requirements and the design of PI controller for EV aggregators participating in frequency regulation service. Future studies may include the computation of stability delay margin of multi-area LFC systems with multiple EV aggregators with incommensurate time delays using advanced clustering with frequency sweeping (ACFS) [27], [28], and the design of PI controller.

Appendix A

The coefficients of $P(s)$ and $Q(s)$ polynomials in (3) are given as:

$$\begin{cases} p_6 = MRT_gT_rT_cT_{EV} \\ p_5 = DRT_gT_rT_cT_{EV} + MR(T_gT_rT_c + T_rT_cT_{EV} + T_gT_cT_{EV} + T_gT_rT_{EV}) \\ p_4 = DR(T_gT_rT_c + T_rT_cT_{EV} + T_gT_cT_{EV} + T_gT_rT_{EV}) + \\ \quad MR(T_rT_c + T_gT_c + T_gT_r + T_cT_{EV} + T_rT_{EV} + T_gT_{EV}) \\ p_3 = DR(T_rT_c + T_gT_c + T_gT_r + T_cT_{EV} + T_rT_{EV} + T_gT_{EV}) + \\ \quad MR(T_c + T_r + T_g + T_{EV}) + F_pT_rT_{EV} + \alpha_0\beta RK_pF_pT_rT_{EV} \\ p_2 = DR(T_c + T_r + T_g + T_{EV}) + MR + F_pT_r + T_{EV} + \\ \quad \alpha_0\beta R(K_pT_{EV} + K_pF_pT_r + K_IF_pT_rT_{EV}) \\ p_1 = DR + 1 + \alpha_0\beta R(K_p + K_IT_{EV} + K_IF_pT_r) \\ p_0 = \alpha_0\beta RK_I \end{cases} \quad \text{(A1)}$$

$$\begin{cases} q_4 = \alpha_1 \beta R K_{EV} K_p T_g T_r T_c \\ q_3 = \alpha_1 \beta R K_{EV} (K_p T_r T_c + K_p T_g T_c + K_p T_g T_r + K_I T_g T_r T_c) \\ q_2 = \alpha_1 \beta R K_{EV} (K_p T_c + K_p T_r + K_p T_g + K_I T_r T_c + K_I T_g T_c + K_I T_g T_r) \\ q_1 = \alpha_1 \beta R K_{EV} (K_p + K_I T_c + K_I T_r + K_I T_g) \\ q_0 = \alpha_1 \beta R K_{EV} K_I \end{cases} \tag{A2}$$

The coefficients $A_1(\omega_c)$, $B_1(\omega_c)$, $C_1(\omega_c)$ and $A_2(\omega_c)$, $B_2(\omega_c)$, $C_2(\omega_c)$ shown in (6) are given as:

$$\begin{cases} A_1(\omega_c) = -p_2' \omega_c^2 + q_4' \omega_c^4 \cos(\omega_c \tau) - q_2' \omega_c^2 \cos(\omega_c \tau) - \\ \qquad q_3' \omega_c^3 \sin(\omega_c \tau) + q_1' \omega_c \sin(\omega_c \tau) \\ B_1(\omega_c) = -p_2'' \omega_c^2 + p_0'' - q_2'' \omega_c^2 \cos(\omega_c \tau) + q_0'' \cos(\omega_c \tau) - \\ \qquad q_3'' \omega_c^3 \sin(\omega_c \tau) + q_1'' \omega_c \sin(\omega_c \tau) \\ C_1(\omega_c) = -p_6 \omega_c^6 + p_4 \omega_c^4 - p_2 \omega_c^2 \end{cases} \tag{A3}$$

$$\begin{cases} A_2(\omega_c) = -p_3' \omega_c^3 + p_1' \omega_c - q_3' \omega_c^3 \cos(\omega_c \tau) + \\ \qquad q_4' \omega_c^4 \sin(\omega_c \tau) + q_2' \omega_c^2 \sin(\omega_c \tau) \\ B_2(\omega_c) = p_1'' \omega_c - q_3'' \omega_c^3 \cos(\omega_c \tau) + q_1'' \omega_c \cos(\omega_c \tau) + \\ \qquad q_2'' \omega_c^2 \sin(\omega_c \tau) - q_0'' \sin(\omega_c \tau) \\ C_2(\omega_c) = p_5 \omega_c^5 - p_3 \omega_c^3 + p_1 \omega_c \end{cases} \tag{A4}$$

REFERENCES

[1] P. S. Kundur, *Power System Stability and Control*. New York: McGraw-Hill, 1994.

[2] H. Bevrani, A. Ghosh, and G. Ledwich, "Renewable energy sources and frequency regulation: survey and new perspectives," *IET Renewable Power Generation*, vol. 4, no. 5, pp. 438-457, Sept. 2010.

[3] W. Kempton and S. Letendre, "Electric vehicles as a new power source for electric utilities," *Transportation Research Part D*, vol. 2, no. 3, pp.157-175, Sept. 1997.

[4] J. R. Pillai and B. Bak-Jensen, "Integration of vehicle-to-grid in the western Danish power system," *IEEE Transactions on Sustainable Energy*, vol. 2, no. 1, pp. 12-19, Jan. 2011.

[5] M. Mu, J. Wu, J. Ekanayake *et al*., "Primary frequency response from electric vehicles in the Great Britain power system," *IEEE Transactions on Smart Grid*, vol. 4, no. 2, pp. 1142-1150, Jun. 2013.

[6] C. Guille and G. Gross, "A conceptual framework for the vehicle-to-grid (V2G) implementation," *Energy Policy*, vol. 37, no. 11, pp. 4379-4390, Nov. 2009.

[7] S. Han, S. Han, and K. Sezaki, "Development of an optimal vehicle-to-grid aggregator for frequency regulation," *IEEE Transactions on Smart Grid*, vol. 1, no. 1, pp. 65-72, Jun. 2010.

[8] R. J. Bessa and M. A. Matos, "The role of an aggregator agent for EV in the electrical market," in *Proceedings of 7th Mediterranean Conference and Exhibition on Power Generation, Transmission, Distribution and Energy Conversion*, Agia Napa, Cyprus, Nov. 2010, pp. 7-10.

[9] R. J. Bessa, M. A. Matos, and F. J. Soares, "Framework for the participation of EV aggregators in the electricity market," in *Proceedings of 2014 IEEE International Electric Vehicle Conference (IEVC)*, Florence, Italy, Dec. 2014, pp. 1-8.

[10] A. M. Carreiroa, H. M. Jorge, and C. H. Antunesa, "Energy management systems aggregators: a literature survey," *Renewable and Sustainable Energy Reviews*, vol. 73, pp. 1160-1172, Jun. 2017.

[11] C. Quinn, D. Zimmerle, and T. H. Bradley, "The effect of communication architecture on the availability, reliability, and economics of plug-in hybrid electric vehicle-to-grid ancillary services," *Journal of Power Sources*, vol. 195, no. 5, pp. 1500-1509, Mar. 2010.

[12] K. Ko and D. K. Sung, "The Effect of cellular network-based communication delays in an EV aggregator's domain on frequency regulation service," *IEEE Transactions on Smart Grid*, vol. 10, no. 1, pp. 65-73, Jan. 2019.

[13] K. Mak and B. L. Holland, "Migrating electrical power network SCADA systems to TCP/IP and ethernet networking," *Power Engineering Journal*, vol. 16, no. 6, pp. 305-311, Dec. 2002.

[14] K. S. Ko and D. K. Sung, "The effect of EV aggregators with time-varying delays on the stability of a load frequency control system," *IEEE Transactions on Power Systems*, vol. 33, no. 1, pp. 669-680, Jan. 2018.

[15] A. Khalil and A. S. Peng, "Delay margin computation for load frequency control system with plug-in electric vehicles," *International Journal of Power and Energy Systems*, vol. 38, no. 3, pp. 1-17, Mar. 2017.

[16] E. Yao, V. W. Wong, and R. Schober, "Robust frequency regulation capacity scheduling algorithm for electric vehicles," *IEEE Transactions on Smart Grid*, vol. 8, no. 2, pp. 984-997, Mar. 2017.

[17] A. Bilh, K. Naik, and R. El-Shatshat, "Evaluating electric vehicles' response time to regulation signals in smart grids," *IEEE Transactions on Industrial Informatics*, vol. 14, no. 3, pp. 1210-1219, Mar. 2018.

[18] N. Tan, I. Kaya, C. Yeroğlu *et al*., "Computation of stabilizing PI and PID controllers using the stability boundary locus," *Energy Conversion and Management*, vol. 47, no. 18-19, pp. 3045-3058, Nov. 2006.

[19] Ş. Sönmez and S. Ayasun, "Stability region in the parameter space of PI controller for a single-area load frequency control system with time delay," *IEEE Transactions on Power Systems*, vol. 31, no. 1, pp. 829-830, Jan. 2016.

[20] Ş. Sönmez and S. Ayasun, "Computation of PI controllers ensuring desired gain and phase margins for two-area load frequency control system with communication time delays," *Electric Power Components and Systems*, vol. 46, no. 8, pp. 938-947, Oct. 2018.

[21] K. E. Walton and J. E. Marshall, "Direct method for TDS stability analysis," *IEE Proceeding Part D*, vol. 134, no. 2, pp.101-107, Mar. 1987.

[22] Ş. Sönmez, S. Ayasun, and C. O. Nwankpa, "An exact method for computing delay margin for stability of load frequency control systems with constant communication delays," *IEEE Transactions on Power Systems*, vol. 31, no. 1, pp. 370-377, Jan. 2016.

[23] *Model-based and System-based Design Using Simulink*, The MathWorks, Natick, 2000.

[24] T. Vyhlídal and P. Zítek, "Mapping based algorithm for large-scale computation of quasi-polynomial zeros," *IEEE Transactions on Automatic Control*, vol. 54, no. 1, pp. 171-177, Jan. 2009.

[25] K. S. Ko, S. Han, and D. K. Sung, "A new mileage payment for EV aggregators with varying delays in frequency regulation service," *IEEE Transactions on Smart Grid*, vol. 9, no. 4, pp. 2616-2624, Jul. 2018.

[26] H. Fan, L. Jiang, C. K. Zhang *et al*., "Frequency regulation of multi-area power systems with plug-in electric vehicles considering communication delays," *IET Generation, Transmission & Distribution*, vol. 10, no. 14, pp. 3481-3491, Nov. 2016.

[27] R. Sipahi and I. I. Delice, "Advanced clustering with frequency sweeping methodology for the stability analysis of multiple time-delay systems," *IEEE Transactions on Automatic Control*, vol. 56, no. 2, pp. 467-472, Feb. 2011.

[28] I. I. Delice and R. Sipahi, "Delay-independent stability test for systems with multiple time-delays," *IEEE Transactions on Automatic Control*, vol. 57, no. 4, pp. 963-972, Apr. 2012.

Ausnain Naveed received the B.E. degree in electrical engineering from Bahria University, Islamabad, Pakistan, in 2012, and the M.Sc. degree in electrical and electronic engineering from University of Leicester, Leicestershire, UK, in 2014. He is currently pursuing the Ph.D. degree in electrical and electronic engineering in Niğde Ömer Halisdemir University, Niğde, Turkey. His research interests include modeling and stability analysis of time delayed dynamical systems, control solutions for integrated energy systems and power system dynamics.

Şahin Sönmez received the B.Sc. degree in electrical and electronic engineering from Fırat University, Elazig, Turkey, in 2010, the M.Sc. and Ph.D. degrees in electrical and electronic engineering from Niğde Ömer Halisdemir University, Niğde, Turkey, in 2013 and 2017, respectively. He is currently working as an Assistant Professor in the same department. His research interests include modeling and stability analysis of time delayed dynamical systems, power system dynamics and control.

Saffet Ayasun received the B.Sc. degree in electrical and electronic engineering from Gazi University, Ankara, Turkey, in 1989, the M.Sc. and Ph.D. degrees in electrical power engineering from Drexel University, Philadelphia, USA, in 1997 and 2001, respectively. He is currently working as a Professor in Gazi University, Ankara, Turkey. His research interests include power system dynamics, voltage stability, bifurcation theory and its applications to electrical power systems, modeling and stability analysis of time delayed dynamical systems.